J Fluoresc (2015) 25:675–684
DOI 10.1007/s10895-015-1553-x

ORIGINAL PAPER

Phenazine Fused Benzo Coumarins with Negative Solvatochromism and Positive Solvatochromic Emission - Synthesis, Photo Physical Properties, DFT and TDDFT Studies

Amol S. Choudhary · Nagaiyan Sekar

Received: 6 December 2014 / Accepted: 5 March 2015 / Published online: 14 March 2015

Abstract 5-Hydroxybenzo[a]phenazine-6-carbaldehyde was synthesized and condensed with substituted active methylene compounds to obtain four novel phenazine fused coumarin dyes. Solutions of imidazole containing dyes in various solvents exhibited yellow to orange fluorescence while benzothiazole containing dyes showed brilliant bluish green fluorescence. The dyes showed pronounced negative solvatochromism. However, the emission experienced progressive red shift with increasing polarity. The excited states of these dyes are proved to be more polar than the ground state. The dyes showed fairly good quantum yield in the range 0.1-0.7, and displayed high thermal stability, as determined using thermo gravimetric analysis. The density functional theory computations showed that intramolecular charge transfer occurs from the 3 position to the 7 position. The excited state computation using time dependent functional theory predicted the emission well.

Keywords 5, 6 and 7, 8 fused coumarins · Phenazine · Solvatochromisms · Fluorescence · Charge transfer

Introduction

Substituted coumarins having good emission quantum yield, photo stability and solubility in organic solvents represent an important class of fluorophores [1, 2]. They are used in tunable dye lasers [3, 4], fluorescent markers [5–7], organic light emitting diodes (OLEDs) [8], photosensitizer [9] and dye sensitized solar cells (DSSC) [10]. 3-Aryl and 3-hetaryl coumarins are visualized as the trans-fixed stilbenes, the strong fluorescence of which is ascribed to the charge transfer from the styryl to the carbonyloxy group. The absorption and emission characteristics of coumarin are altered by the nature and position of the substituents in the coumarin ring as well as the microenvironment like polarity and viscosity. Electron withdrawing groups in the 3-position and electron donating groups in the 5 and 7 positions have been shown to enhance the conjugation bringing about a red shift in the absorption and hence emission [11]. The photophysical properties of 7-donor substituted coumarins are fairly well studied [11] especially the solvatochromic properties in the context of designing molecular probes [11–14]. Coumarin molecules with 6, 7-fused benzene ring have been synthesized [12–18] and it has been found that the 6, 7-benzo-fused coumarin has a blue shifted absorption compared to the 7-donor substituted coumarins. There are also some reports on the potentially biologically active 5, 6- and 7, 8- fused coumarins [19, 20], the photophysical properties of which have not been studied.

It is quite likely that 5,6- and 7,8-beznzo fused coumarins would have strong emission and the photophysical characteristics would arise from a π-π* interactions rather than the n- π * interaction prominent in the 7-donor substituted coumarins. With this in mind we report here for the first time the synthesis of coumarin core with 5, 6- phenazine fusion and 7, 8-benzofusion. It was envisaged that the phenazine fused core will act as π - acceptor in the overall conjugated system (Fig. 1).

This polyfunctionalized heterocyclic coumarins analogues can be regarded as a rigidized 2-(benzo[d]thiazol-2-yl)-3H-

A. S. Choudhary · N. Sekar (✉)
Tinctorial Chemistry Group, Department of dyestuff and intermediate Technology, Institute of Chemical Technology, Mumbai, Nathalal Parekh Marg, Matunga, Mumbai 400 019, India
e-mail: n.sekar@ictmumbai.edu.in

N. Sekar
e-mail: nethi.sekar@gmail.com

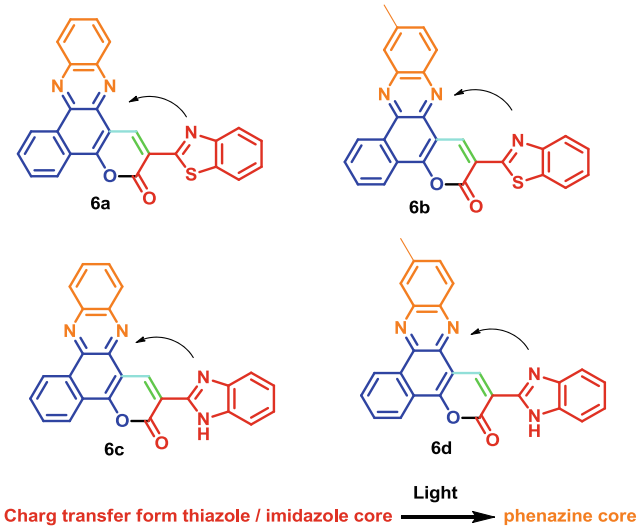

Fig. 1 Synthesized 5, 6 and 7, 8 fused coumarin **6a-6d**

benzo[a]pyrano[2,3-c] phenazin-3-one with a fusion of phenazine and napthacoumarin moieties. The absorption emission properties of the newly synthesized bis annulated coumarins have been studied and compared with the values obtained from Density Functional Theory (DFT) and Time Dependent DFT (TD-DFT) computations. DFT computations were carried out to study the geometrical and electronic properties of the synthesized molecules. The experimental UV–vis and emission spectra were interpreted with the help of TD-DFT computations and the bulk solvent effects were studied using the polarized continuum model (PCM) [21, 22].

Materials and Methods

2-Hydroxy-1, 4-napthaquinone, substituted o-phenylenediamine, o-aminothiophenol, and malononitrile were procured from Sigma Aldrich. 2-Cyanomethylbenzimidazole and 2-cyanomethylbenzothiazole were synthesized by the reported method [23]. The reaction was monitored by TLC using 0.25 mm E-Merck silica gel 60F254 percolated plates, which were visualized with UV light. Melting points were measured on standard melting point apparatus from Sunder industrial product Mumbai, and are uncorrected. The FTIR spectra were recorded on a Perkin-Elmer Spectrum 100 FTIR Spectrometer. ^{1}HNMR spectra were recorded on VXR 500 MHz instrument using TMS as an internal standard. The visible absorption spectra of the compounds were recorded on a Spectronic Genesys 2 UV-Visible spectrophotometer. The emission and excitation spectra of the compounds were measured on Varian Cary eclipse spectrofluorimeter. Simultaneous DSC-TGA measurements were performed out on SDT Q600 v8.2 Build 100 model of TA instruments Waters (India) Pvt. Ltd.

Synthesis and Characterization

General Method for the Synthesis and Characterization of **3a-3b**

2-Hydroxy-1, 4-napthaquinone 1 (2 mol) and substituted o-phenylenediamine **2a-2d** (2 mol) were stirred in a mixture of AcOH: EtOH (50:50) (20 ml) at 80 °C for 1–1.5 h. The reaction was monitored by TLC. After completion of the reaction, the reaction mass was poured in to the crushed ice and stirred for 30 min at room temperature. The reaction mass was filtered and the product was purified by column chromatography using silica gel 100–200 mesh and ethyl acetate: hexane (50:50) as eluent system.

General Method for the Synthesis of **4a-4b**

$POCl_3$ (0.015 mol) was added to DMF (0.20 mol) at 0 °C within 15 min and stirred for 30 min at 0 °C. Naphtho[1,2-a]phenazin-5-ol 3a-3b (0.01 mol) dissolved in DMF (5 ml) was added slowly at 0–5 °C and stirred for 30 min. The reaction mixture was then heated to 80–90 °C for 2–3 h and the reaction was monitored by TLC. The reaction mass was poured in ice and stirred neutralized with sodium bicarbonate, filtered and dried. The crude aldehyde was recrystallized from ethanol.

Synthesis of 5-hydroxy-10-methylbenzo[a] phenazine-6-carbaldehyde **4a**

Yield = 55 %, Melting point: 173–177 °C, FT-IR (KBr, cm^{-1}): 3100 (−OH), 2930 (HC = O), 1600 (C = O), 1577 (C = N), 1200 (C-O). ^{1}HNMR ($CDCl_3$, 500 MHz)=δ 2.67 (s, 3H, $-CH_3$), 7.83 (m, 4H, J=7.4, 5.1 Hz, Ar-H), 7.29 (m, 4H, Ar-H), 8.60 (bs, 1H, −OH), 8.5 (s, 1H) ppm. Mass: m/z 288.24 [M+1].

Synthesis of 5-hydroxybenzo[a]phenazine-6-carbaldehyde **4b**

Yield = 59 %, Melting point: 163–168 0C FT-IR (KBr, cm-1): 3100 (−OH), 2930 (HC = O), 1600 (C = O), 1577 (C = N), 1200 (C-O). ^{1}HNMR ($CDCl_3$, 500 MHz) = δ 7.782 (dd, 4H, J = 6.9, 4.7 Hz, Ar-H), 7.212 (dd, 4H, J = 7.4, 5.1 Hz, Ar-H), 8.60 (bs, 1H,-OH), δ 8.2 (s, 1H, Aldehyde -CHO) ppm. Mass: m/z 274.13 [M+1].

Synthesis of 2-(benzo[d]thiazol-2-yl)-3H-benzo[a]pyrano [2, 3-c] phenazin-3-one **6a-6d**

5-Hydroxybenzo[a]phenazine-6-carbaldehyde 4a-4b (1.8 mmol) and 2-cyanomethyl-1, 3-benzothiazole **5a** or 2-cyanomethyl-1,3-benzoimidazole **5b** (2.0 mmol) was stirred in ethanol (20 ml). A catalytic amount of piperidine was added

to the mixture and refluxed for 2 h. The reaction was monitored by TLC. The yellow coloured compound precipitated out was filtered and purified by column chromatography using silica 100–200 mesh and ethyl acetate: hexane as the eluent.

Synthesis of 2-(benzo[d]thiazol-2-yl)-12-methyl-3H-benzo[a] pyrano[2,3-c]phenazin- 3-one **6a**

Yield = 81 %; Melting point = 278–280 °C. FT-IR (cm^{-1}) = 1701 (C = O), 1582 (C = C, aromatic). ^{1}HNMR (CDCl3, 500 MHz) = δ 8.247−7.972 (m, 4H, J = 7.3 Hz), δ 7.525−7.499 (m, 3H, overlapped, Ar-H), δ 8.415 (s, 1H, lactone ring H), δ 7.63−7.41 (m, 4H, overlapped, Ar-H), δ 2.514 (s, 3H, $-CH_3$). Mass = m/z 445.63 (M+1).

Synthesis of 2-(benzo[d]thiazol-2-yl)-3H-benzo[a] pyrano[2,3-c]phenazin-3-one **6b**

Yield = 78 %; Melting point = 270–272 °C. FT-IR (cm^{-1}) = 1701 (C = O), 1582 (C = C, aromatic). ^{1}HNMR (CDCl3¬¬, 300 MHz) = δ 8.237−7.992 (m, 4H, J=6.9 Hz), δ 7.532−7.012 (m, 4H, overlapped, Ar-H), δ 8.417 (s, 1H, lactone ring H), δ 7.636−7.418 (m, 4H, overlapped, Ar-H). Mass = m/z 431.52 (M+1).

Synthesis of 2-(1H-benzo[d]imidazol-2-yl) -12-methyl-3H-benzo[a]pyrano[2,3-c] phenazin-3-one **6c**

Yield = 71 %; Melting point = 280–283 °C. FT-IR (cm^{-1}) = 1701 (C = O), 1582 (C = C, aromatic). ^{1}HNMR ($CDCl_3$, 500 MHz) = δ 9.24 (bs, 1H, −NH) 8.68 (s, 1H, lactone ring H), δ 8.329−8.114 (dd, 3H, J=7.6 Hz), δ 7.217−7.012 (m, 4H, overlapped, Ar-H), δ 7.221−7.018 (m, 4H, overlapped, Ar-H), δ 2.473 (s, 3H, $-CH_3$). Mass = m/z 428.05 (M+1).

Synthesis of 2-(1H-benzo[d]imidazol-2-yl)-3H-benzo[a] pyrano[2,3-c]phenazin-3-one **6d**

Yield = 84 %; Melting point = 278–280 °C. FT-IR (cm-1) = 1701 cm^{-1} (C = O), 1582 cm^{-1} (C = C, aromatic). Mass = m/z 383 (M+1). ^{1}HNMR ($CDCl_3$, 500 MHz) = 1H NMR ($CDCl_3$, 300 MHz) = δ 9.254 (bs, 1H, −NH) 8.71 (s, 1H, lactone ring H), δ 8.211−8.025 (dd, 4H, J=7.3 Hz), δ 7.214−7.091 (m, 4H, overlapped, Ar-H), δ 7.221−7.018 (m, 4H, overlapped, Ar-H). Mass = m/z 414.23 (M+1).

Computation Strategy

All the computations were performed using the Gaussian 09 program package [24]. The optimization of the ground state (S0) geometry of the dyes was done using DFT [25] method. The functional used was B3LYP, (the B3LYP combines Becke's three parameter exchange functional (B3) [26] with the nonlocal correlation functional by Lee, Yang and Parr (LYP) [27]). The basis set used in both, DFT and TD-DFT methods for all the atoms was 6-31G(d). The frequency computations were performed at the same level of theory in order to verify whether the optimised structures have minimum energy. The vertical excitation energies and oscillator strengths were obtained for the 20 lowest S0-S1 transitions at the optimized ground state equilibrium geometries by using the TD-DFT using the same hybrid functional and basis set [28–34]. To obtain their minimum energy geometries (which correspond to the emissive state) the low-lying first singlet excited states (S1) of the dyes were relaxed using the TD-DFT. The energy difference between the optimized geometries at the first singlet excited state and the ground state was used in calculating the emission [35]. The frequency computations were also carried out at the same level of theory on the optimised geometry of the first excited state of the dyes. All the computations in the chloroform media were carried out using the Self-Consistent Reaction Field (SCRF) under the Polarizable Continuum Model (PCM) [21, 22]. The electronic absorption spectra, including wavelengths, oscillators strengths, and main configuration assignment, were systematically investigated using TD-DFT with the PCM model on the basis of the optimized ground structures. The emissions were calculated using TD-DFT from optimised structures in the excited state using the B3LYP/6-31G(d) method.

Results and Discussion

Synthetic Strategy

The coumarin derivatives **6a–6d** were synthesized by following the sequence of reactions illustrated in Scheme 1. 2-Hydroxy-1, 4-napthaquinone **1** was condensed with the substituted 1, 2-diaminobenzenes **2a-2b** in acetic acid to afford benzo[a]phenazin-5-ol **3a-3b** in excellent yield. The electron rich benzo[a]phenazin-5-ol **3a-3b** derivatives were subjected to formylation reaction under Vilsmeier–Haack conditions to obtain 5-hydroxybenzo[a]phenazine-6-carbaldehyde **4a-4b**

The condensation of **4a-4b** with the active methylene compounds **5a-5b** under Knoevenagel conditions followed by an intramolecular cyclization gave **6a-6d**. A mixture of the aldehyde **4a-4b** and appropriate active methylene compounds **5a-5b** was refluxed in absolute ethanol containing a catalytic amount of piperidine to yield the imino coumarin derivatives which on hydrolysis gave the coumarins **6a–6d**

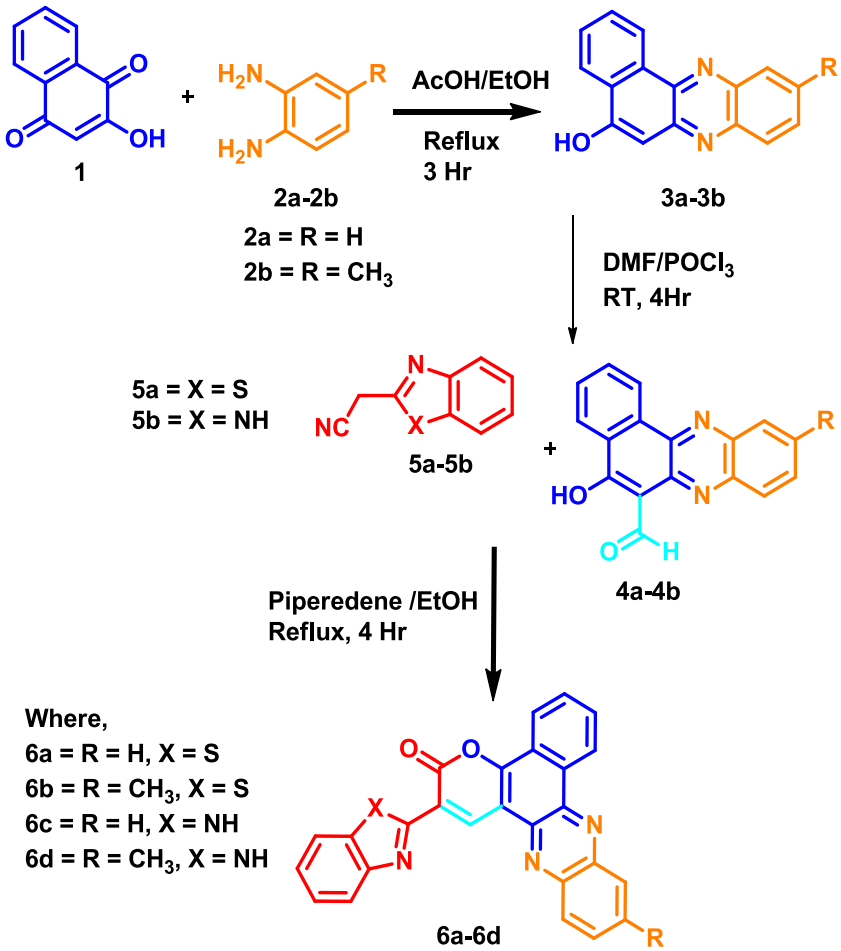

Scheme 1 Synthesis of 5-hydroxybenzo[a]phenazine-6-carbaldehyde (4a-4b) and 2-(1H-benzo[d] imidazol-2-yl)-3H-benzo[a]pyrano[2,3-c]phenazin-3-one (6a-6d)

Table 1 Absorption maxima wavelength (λabs, nm), absorbance (a.u), fluorescence emission maxima wavelength (λems, nm); fluorescence quantum yield (Φf) and Stokes shift (nm) of synthesized dyes **6a-6d** in different solvents

Solvent	Absorption and emission of Compound 6a-6d											
	6a			6b			6c			6d		
	λ_{abs} (ε_{max})	λ_{ems} (Φ_f)	[a] Δλ	λ_{abs} (ε_{max})	λ_{ems} (Φ_f)	[a] Δλ	λ_{abs} (ε_{max})	λ_{ems} (Φ_f)	[a] Δλ	λ_{abs} (ε_{max})	λ_{ems} (Φ_f)	[a] Δλ
Toluene	449 (0.513)	474 (0.71)	36	452 (0.782)	(0.660)	51	499 (0.69)	532 (0.073)	33	470 (0.403)	519 (0.061)	49
THF	443 (0.543)	484 (0.731)	39	454 (0.737)	512 (0.663)	58	490 (0.687)	530 (0.064)	40	456 (0.483)	523 (0.058)	67
Hexane	455 (0.562)	470 (0.741)	30	455 (0.379)	501 (0.651)	46	504 (0.613)	533 (0.009)	29	465 (0.497)	517 (0.061)	52
ACN	443 (0.603)	509 (0.695)	20	443 (0.1372)	489 (0.309)	46	478 (0.598)	545 (0.098)	67	448 (0.301)	535 (0.058)	87
MeOH	443 (0.65)	499 (0.614)	25	438 (0.1673)	486 (0.587)	48	461 (0.56)	525 (0.099)	51	490 (0.384)	548 (0.067)	58
$CHCl_3$	452 (0.652)	490 (0.634)	20	440 (0.4326)	493 (0.601)	53	449 (0.55)	521 (0.103)	72	460 (0.637)	537 (0.351)	77
DCM	467 (0.654)	493 (0.691)	26	441 (0.4592)	497 (0.696)	56	478 (0.61)	521 (0.141)	43	456 (0.617)	540 (0.073)	84
Acetone	442 (0.542)	498 (0.602)	35	443 (0.3803)	507 (0.477)	64	473 (0.492)	509 (0.104)	36	451 (0.44)	521 (0.25)	70
DMF	440 (0.586)	509 (0.197)	79	442 (0.1682)	533 (0.184)	91	474 (0.185)	545 (0.134)	71	452 (0.687)	560 (0.193)	108
EtOH	442 (0.65)	509 (0.603)	19	437 (0.4505)	484 (0.536)	47	475 (0.598)	526 (0.096)	51	450 (0.682)	543 (0.064	93
DMSO	440 (0.584)	513 (0.189)	76	439 (0.1671)	514 (0.163)	75	475 (0.174)	551 (0.047)	76	450 (0.69)	557 (0.187)	107

[a] Δλ = Stoke shift = [(Absorption wavelength (nm) – Emission Wavelength (nm)]

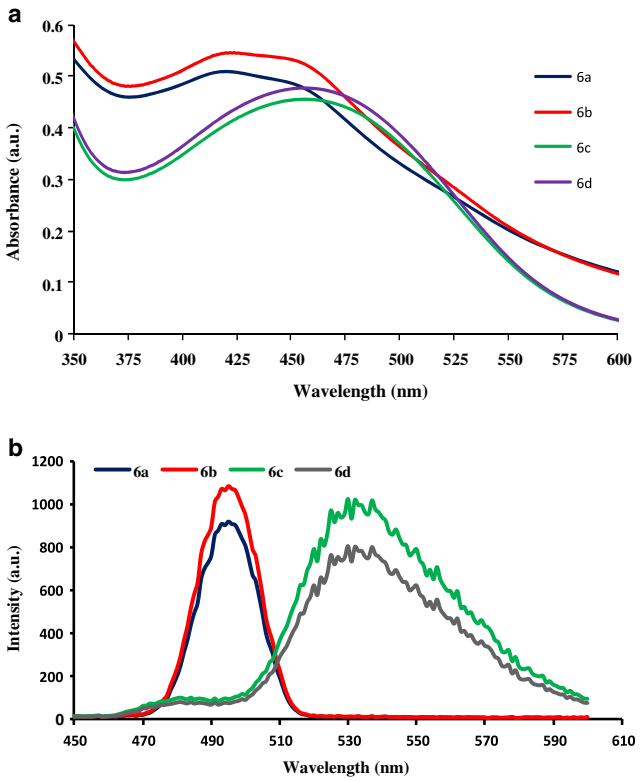

Fig. 2 **a**. UV–vis absorption spectra of compounds **6a**, **6b**, **6c** and **6d**. C = 1.0×10^{-5} mol dm^{-3} in chloroform. 20 °C. **b.** Emission spectra of compounds **6a**, **6b**, **6c** and **6d**. C = 1.0×10^{-5} mol dm^{-3} in chloroform, 20 °C

Photophysical Characteristics of the Dyes **6a-6d**

Effects of Polarity on the Absorption Properties of the Dyes 6a-6d

To investigate the influence of polarity on the absorption maxima of the dyes **6a-6d**, their absorption spectra were measured in solvents of different polarity. The absorption (λ_{max}), and emission (λ_{ems}) spectral characteristics of the synthesized dyes **6a**, **6b**, **6c** and **6d** measured in different solvents are presented in Table 1

The electronic absorption spectra of the dyes **6a-6d** dyes in chloroform displayed absorption maxima in the visible region from 430 to 480 nm and the emission range is found to be 470 to 560 nm depending on the nature of substituent group (Fig. 2a and b). All the dyes **6a-6d** show slight negative solvatochromism (Table 1). The absorption is red shifted in non-polar solvents compared to polar solvents. This fact is also supported by the DFT computations. An increase in the polarity brings about an increasing in the band gap for the dyes **6a** and **6c** (Table 2).

The computational studies reveal that both HOMO and LUMO are stabilized more in polar solvents than in nonpolar solvents. However, the compound **6a** shows bathochromic shift as compared to the compound **6b** in both the polar and nonpolar solvents. Similarly the compound **6c** showed a bathochromic shift as compared to the compound **6d**. The dyes having benzimidazole core **6c** and **6d** showed bathochromic shift as compared to the dyes having benzothiazole **6a** and **6b** (Table 1 and Fig. 2a and b).

Effects of Polarity on the Emission Spectra of the Dyes **6a-6d**

Polarity of the solvents have appreciable influence on the emission properties of the molecules. The emission properties of **6a-6d** in different solvents are shown in Table 1. As the polarity of solvent increases emission experiences red shift. The compound **6a-6d** show red shifted emission in DMF and DMSO as compared to the emissions in hexane, toluene, MeOH, CH_3COCH_3 and CH_2Cl_2 (Table 1).

Table 2 Calculated band gap of compounds **6a** and **6c** in different solvents

Solvents	Dye 6a				Dye 6c			
	Energy [a]	Energy [a] (H) HOMO	Energy [a] LUMO	[b]Δ Band gap [a]	Energy [a]	Energy [a] HOMO	Energy [a] LUMO	[b]Δ Band gap [a]
Gas	−1750.8726	−0.21228	−0.09751	0.11477	−1408.0474	−0.20388	−0.09605	0.10783
n-Hexane	−1750.8768	−0.21463	−0.09844	0.11619	−1408.0523	−0.20734	−0.09662	0.11072
Toluene	−1750.8781	−0.21536	−0.09883	0.11653	−1408.0532	−0.20794	−0.09677	0.11117
$CHCl_3$	−1750.8812	−0.21702	−0.09982	0.1172	−1408.0564	−0.21003	−0.09742	0.11261
THF	−1750.8825	−0.21774	−0.10029	0.11745	−1408.0579	−0.21094	−0.09775	0.11319
DCM	−1750.8830	−0.21796	−0.10045	0.11751	−1408.0583	−0.21121	−0.09785	0.11336
Acetone	−1750.8843	−0.21860	−0.10090	0.1177	−1408.0597	−0.21201	−0.09816	0.11385
Ethanol	−1750.8844	−0.21869	−0.10096	0.11773	−1408.0599	−0.21213	−0.09821	0.11392
Methanol	−1750.8846	−0.21879	−0.10104	0.11775	−1408.0601	−0.21225	−0.09826	0.11399
ACN	−1750.8847	−0.21882	−0.10106	0.11776	−1408.0602	−0.21229	−0.09827	0.11402
DMF	−1750.8847	−0.21883	−0.10107	0.11776	−1408.0601	−0.21224	−0.09789	0.11435
DMSO	−1750.8849	−0.21889	−0.10111	0.11778	−1408.0603	−0.21238	−0.09831	0.11407

[a] Energy in Hartree (H)

Table 3 Calculated ground state and excited state ratio of dye **6a** and **6d**

Solvents	Dipole moment 6a			Dipole moment 6d		
	[c] u_g	[d] u_e	[e] u_e/u_g	[c] u_g	[d] u_e	[e] ratio u_e/u_g
Toluene	**6.798**	6.685	0.98343606	**5.861**	5.174	0.8828
THF	**6.774**	7.375	1.08871765	**5.845**	5.635	0.9642
hexane	**6.384**	6.474	1.01422417	**5.570**	5.033	0.9036
Acetonitrile	**6.807**	7.699	1.13096235	**5.775**	5.861	1.0149
Methanol	**6.604**	7.690	1.16449122	**5.729**	5.855	1.0220
Chloroform	**5.983**	7.165	1.19751312	**5.271**	5.493	1.0420
DCM	**5.797**	7.441	1.28359239	**5.179**	5.680	1.0968
Acetone	**6.805**	7.632	1.12166948	**5.865**	5.814	0.9912
DMF	**6.552**	7.703	1.17553873	**5.693**	5.864	1.0299
Ethanol	**6.753**	7.660	1.13416946	**5.831**	5.833	1.0004
DMSO	**6.821**	7.721	1.13187023	**5.876**	5.876	1.0001

ug = Ground state dipole moment; u_e = Excited state dipole moment
u_e/u_g = Excited state dipole moment/ Ground state dipole moment

This is due to the fact that the excited state is more polar than the ground state. Estimation of the ratio of the excited state to the ground state dipole moments (ue/ug) using Lippert-Mataga equation showed that the ratio is always more than one (Table 3). Combined DFT and TDDFT computations also showed that the excited state is more polar than the ground state (Table 3).

Effects of Polarity on the Quantum Yield of the Dyes **6a-6d**

The fluorescence quantum yields of the synthesized dyes **6a-6d** were determined in different solvents (Table 1). The fluorescence quantum yields of the dyes largely depend on both the nature of the substituent and the solvent polarity. It is observed that decrease in the solvent polarity strongly enhances the fluorescence quantum yield of **6a-6d** (Table 1). The dyes **6a-6d** showed higher quantum efficiencies in non-polar solvents whereas in polar solvents the quantum yield values were invariably found to be very low. These dyes showed less emission intensity in acetonitrile and DMF showing an obvious positive solvatokinetic behavior suggesting

Fig. 3 Fluorescence emission photographs in long UV light of 6a-6d dye in DCM solvent

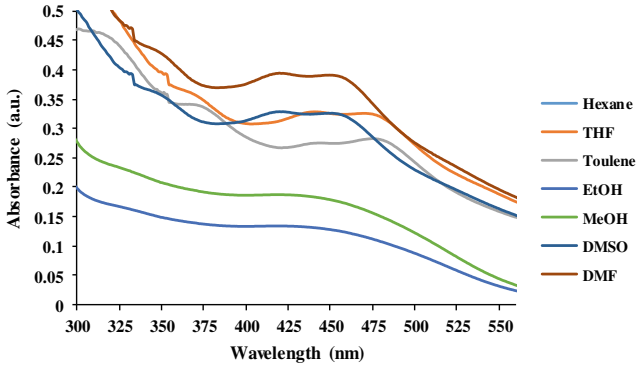

Fig. 4 UV–vis absorption spectra of compound **6a**. C = 1.0×10^{-5} mol dm^{-3} in different polarity of solvent. 20 °C

that a highly polar excited-state population charge transfer state and a non-radiative decay was prominent in these dyes. These fluorescent molecules are blue, green, yellow to dark red in color and soluble in most of the organic solvents. In less polar solvents such as toluene, all the dyes emit blue to orange light of moderate intensity (Fig. 3). On increasing the solvent polarity the emission band also shifts bathochromically and in DMF it emits red light that the fluorescence emission of **6a-6d** dye in DMF solvent and the difference in the emission color can be easily observed by naked eyes (Figs. 4 and 5). These dyes showed very less emission intensity in DMSO and DMF solvents, which is in accordance with the low fluorescence quantum yield observed (Table 1).

Electronic Vertical Excitation Spectra (TDDFT)

Electronic vertical excitations were calculated using TD-B3LYP/6-31G (d) method. The computed vertical excitation spectra associated with their oscillator strengths, composition, and their assignments of the chromophores as well as corresponding experimental absorption wavelengths of the dye **6a** are presented in Table 4.

Increase in solvent polarity brings about blue-shifted absorption with red-shifted emission. The absorption maxima did not show much solvatochromisms, while the emission is very sensitive to solvent polarity for all the four dyes. These

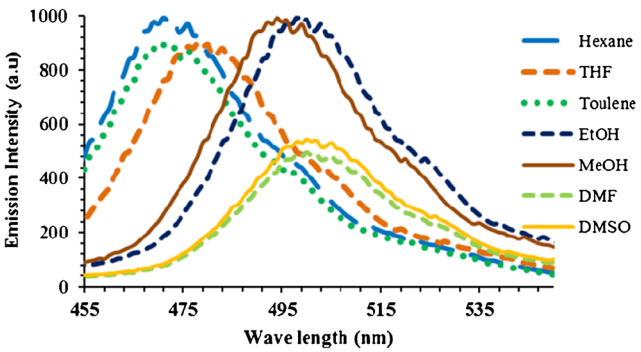

Fig. 5 Emission spectra of compound **6a**. C = 1.0×10^{-5} mol dm^{-3} in different polarity of solvent. 20 °C

Table 4 Calculated vertical excitation of dyes 6a

Solvent	H-L (Ψ^2 %) [a]	Vertical Excitation [b]	f [c]	♂ [d]
DMSO	H-L (97.61)	439.52	0.5547	6.82
DMF	H-L (97.66)	439.78	0.5578	6.81
MeOH	H-L (97.24)	438.32	0.5207	6.80
EtOH	H-L (97.38)	438.95	0.5302	6.77
CAN	H-L (97.31)	438.52	0.5272	6.80
Acetone	H-L (97.37)	439.04	0.5271	6.75
DCM	H-L (97.60)	440.88	0.5330	6.60
CHCl3	H-L (97.63)	442.64	0.5151	6.38
THF	H-L (97.52)	440.95	0.5211	6.55
Hexane	H-L (97.21)	446.68	0.4242	5.80
Toluene	H-L (97.73)	446.44	0.4825	5.98

[a] H-L (Ψ^2 %) = HOMO-LUMO (Orbital contribution %), [b] Vertical excitation unit nm [c] f = oscillator strength [d] ♂ = Dipole moment unit is Debye

observations are attributed to the higher stabilization of the excited states in increasingly polar solvents. The absorption band occurring with higher oscillator strength at lower energy is due to intramolecular charge transfer (ICT) characteristic of $\pi - \pi^*$ transition in the dyes (Fig. 6). The vertical excitation and the emission of the compounds were studied by the TDDFT calculations, based on the ground state (S0) geometry and the optimized excited state (S1) state geometry.

In the case of the dye **6a,** the calculated absorption is at 439.78 nm (Figs. 6 and 7 and Table 5), which is close the experimental results (λabs=440 nm, Table 5). The HOMO-LUMO transition is involved and their orbital contribution is 97 % in the excitation. Both the orbitals are localized on the coumarin framework. The emission of **6a** was also calculated based on the optimized S1 state geometry.

The computed emission wavelength for the dyes **6a** is 502.288 nm, which is in good agreement with the experimental results of 509 nm (Table 5). The benzimidazole core of **6a**, **6b** and benzothiazole core of **6c**, **6d** contributes significantly to the HOMO, whereas the LUMO is more localized on the phenazine fused naptho-coumarin core. This fact reveals that intramolecular charge transfer form thiazole/imidazole core to phenazine core. This is also supported by the fact that the bond length between 19C and 23C was shortened in the excited state and bond angle also was altered (Fig. 7).

There is very little difference observed between the ground state geometry and the S1 state geometry is the dihedral angle, bond angle and bond length between the benzothiazole core and the fused coumarin core. For the ground state (S0 state), the dihedral angle is 0.00230. For the optimized S1 state, the dihedral angle is 0.0, that is, the two units are in coplanar (Figs. 6 and 7). With a very little geometry relaxation a significant variation of the energy levels of LUMO orbital is observed in the case of the dye **6a**. A similar trend was seen

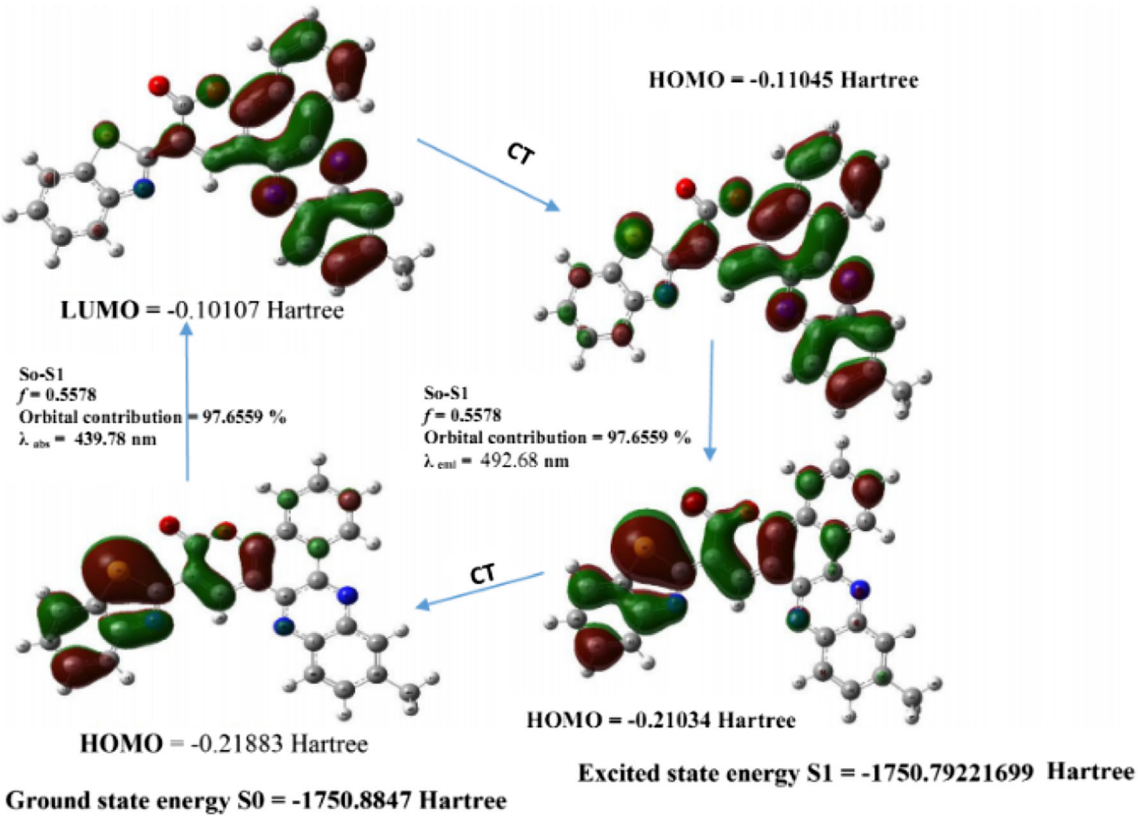

Fig. 6 Optimized geometry parameters of dye **6c** in chloroform solvent in the ground state and excited state

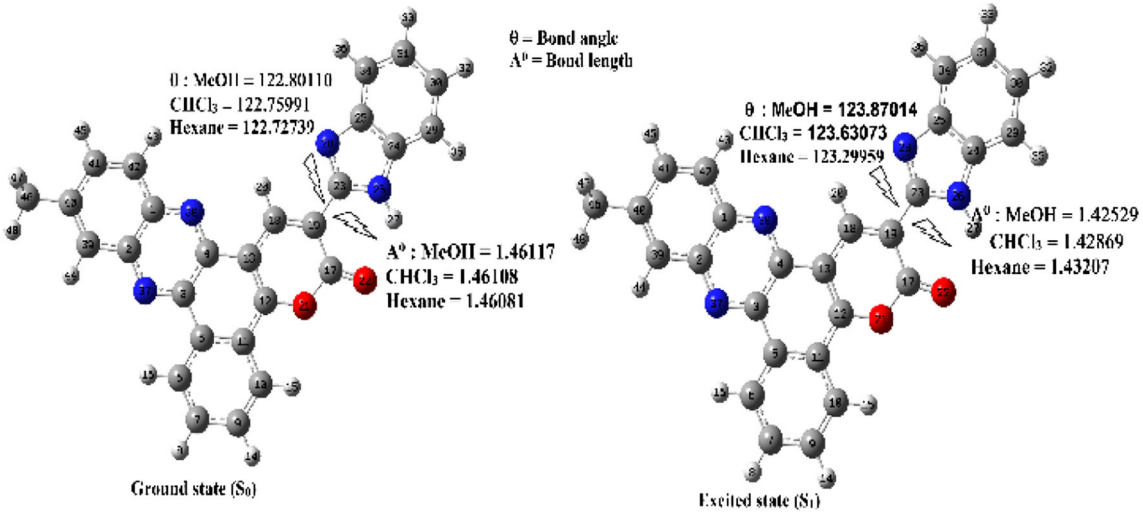

Fig. 7 Thermo gravimetric analysis of compound **6a**, **6b**, **6c** and **6d**

in the dyes **6b**, **6c** and **6d**. These ICT bands for all the four dyes were mainly due to the electronic transition from highest occupied molecular orbital (HOMO) to lowest unoccupied molecular orbital (LUMO).

Thermal Stability of Dyes **6a-6d**

Thermal stability of fluorescent dyes is an essential characteristic deciding their suitability in device applications. In order to give more awareness about the thermal properties of the dyes **6a, 6b, 6c** and **6d**, the thermal studies have been carried out using thermal gravimetric techniques (TGA). The thermo gravimetric studies have been carried out in the temperature range 50–60 °C under nitrogen gas at a heating rate of 10 °C have been carried out using thermal gravimetric techniques (TGA). The thermo gravimetric studies have been carried out in the range 50–600 °C under nitrogen gas at a heating rate of 10 °C min $^{-1}$. The TGA results indicated that the synthesized dyes are stable up to 280 °C which indicates that the rigidisation of coumarin core at position 5, 6 and 7, 8 imparts thermal stability.

TGA revealed the onset decomposition temperature (Td) of dyes 6a,6b, 6c and 6d are 290 0C 92 %), 293 °C (94 %), 297 °C (93 %) and 318 °C (94 %), respectively (Fig. 8) which indicate that the decomposition temperatures increase with the increase of conjugation length and electron rich substituent effect. In general the backbones of these dyes are stable up to 300 °C and above 300 °C the thermo gravimetric curve of these dyes showed a major loss in weight. The comparisons of the Td (decomposition temperature) show that the thermal stability of the **6a, 6b, 6c** and **6d** decreases in the order **6c>6d>6a>6b**. The results showed that synthesized dyes have good thermal stability. Dyes **6a** and **6b** showed a sharp decomposition after temperature 290 °C and 297 °C respectively and completely decomposed beyond 450 °C. The high molecular weight and planer rigid structure of the synthesized dyes are beneficial for intermolecular interactions, such as van der Waals force and dipole-dipole interaction to increase the thermal stability.

Table 5 Experimental UV-Visible absorption (nm), emission (nm) and computed absorption (nm), emission (nm) from TD-B3LYP/6-31G (d) computations for dye **6a** in different solvents

Solvent	[a] λ_{abs} (Experimental)	[b] λ_{abs} (Theoretical)	[c] $\lambda_{emission}$ (Experimental)	[c] $\lambda_{emission(Theoretical)}$
Hexane	455	446.68	470	449.36
Chloroform	452	442.64	484	478.02
THF	443	440.95	484	478.13
Methanol	443	438.32	499	491.95
DMF	440	439.78	509	492.68
DMSO	440	439.52	513	495.99
Ethanol	442	438.95	509	502.29
Acetonitrile	443	438.52	509	512.01
Toluene	449	446.44	474	515.94
DCM	443	440.88	487	516.36
Acetone	442	439.04	498	534.41

[a] Experimental Absorption (nm) [b] Theoretical absorption (nm) [c] Experimental emission (nm) [d] Theoretical absorption (nm)

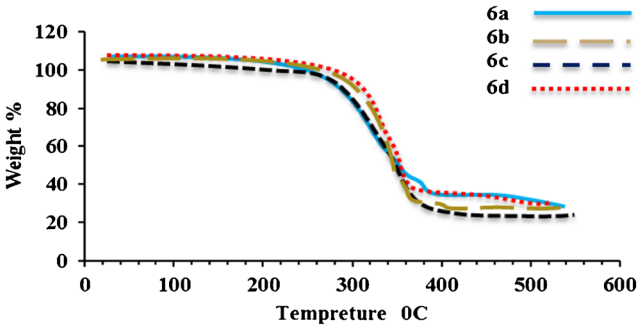

Fig. 8 The frontier MOs involved in the vertical excitation and the emission of coumarin **6b**

Conclusions

In summary, we have synthesized a novel intermediate **4a-4b** and developed an efficient and simple protocol for the synthesis of novel 5, 6-phenazine and 7, 8-benzo fused fluorescent coumarin fluorophores **6a-6d** containing both bipolar phenazine and electron donating benzothiazole/benzimidazole moieties. The synthesized compounds were confirmed by FTIR, ^{1}HNMR, and Mass spectra. Furthermore, these dyes showed the reasonable fluorescence quantum yields (ΦF=0.1–0.78). The fluorescent quantum yield values depend on the substitution. Especially benzothiazolyl derivative shows the good fluorescent quantum as compared to the benzimidazolyl derivative. From the emissive properties, it was concluded that the electronic coupling between D (donor) and A (acceptor) via π-orbital was sufficient to allow a charge transfer (CT) in the molecules. The ICT maximum emission displayed a red shift with an increase in the solvent polarity. The TDDFT calculations show that the new dyes do not undergo significant geometry relaxation upon photo-excitation, which is responsible for the observed small Stokes shifts. Our complementary experimental and theoretical study on the new dyes with novel fused coumarin structure is useful for design of new fluorophores that show desirable photo-physical properties.

Acknowledgements and Ethical Statement Authors are thankful for Indian Institute of Technology, Mumbai for recording NMR and Mass Spectra. Amol Choudhary is thankful to the Centre of Advanced Studies University Grants Commission (CAS-UGC), New Delhi for the financial support by way of SAP fellowship.

References

1. Lin W, Long L, Tan W (2010) A highly sensitive fluorescent probe for detection of benzenethiols in environmental samples and living cells. Chem Commun 46:1503. doi:10.1039/B922478E
2. Lin W, Long L, Feng J, Wang B, Guo C (2007) Synthesis of meso-coumarin-conjugated porphyrins and investigation of their luminescence properties. Eur J Org Chem. 4301. DOI: 10.1002/ejoc.200700475
3. Park S, Kwon J, Kim S, Seo J, Chung K, Park S et al (2009) A white-light-emitting molecule: frustrated energy transfer between constituent emitting centers. J Am Chem Soc 131:14043. doi:10.1021/ja902533f
4. Xu Z, Ding G, Zhong G, Xing G, Li F, Huang W et al (2008) Color tunable organic light-emitting diodes using coumarin dopants. Res Chem Intermed 34:249
5. Chen J, Liu W, Zhou B, Niu G, Zhang H, Wu J, Wang Y, Ju W, Wang P (2013) Coumarin- and rhodamine-fused deep red fluorescent dyes: synthesis, photophysical properties, and bioimaging in vitro. J Org Chem 78:6121. doi:10.1021/jo400783x
6. Zhu S, Lin W, Yuan L (2013) Development of a ratiometric fluorescent pH probe for cell imaging based on a coumarin–quinoline platform. Dyes Pigments 99:465. doi:10.1016/j.dyepig.2013.05.010
7. Zhu S, Lin W, Yuan L (2013) Development of a ratiometric fluorescent pH probe for cell imaging based on a coumarin–quinoline platform. Dyes Pigments 99:465. doi:10.1016/j.snb.2013.03.031
8. Li J, Li X, Wang S (2012) Synthesis, photoluminescent behaviors, and theoretical studies of two novel ketocoumarin derivatives. Spectrochim Acta A Mol Biomol Spectrosc 88:31. doi:10.1016/j.saa.2011.11.044
9. Seo K, Song H, Lee M, Pastore M, Anselmi C, De A et al (2011) Coumarin dyes containing low-band-gap chromophores for dye-sensitised solar cells. Dyes Pigments 90:304. doi:10.1016/j.dyepig.2011.01.009
10. Beyer B, Griese D, Schirrmann C, Pfeifer R, Kahmann S et al (2013) Small molecule bulk heterojunction organic solar cells with coumarin-6 as donor material. Thin Solid Films 536:206. doi:10.1016/j.tsf.2013.03.052
11. Yuan S, Zhang Y, Lu R, Yu A (2013) Photoinduced electron transfer between coumarin dyes and N,N-dimethylaniline in imidazolium based room temperature ionic liquids: effect of the cation's alkyl chain length on the bimolecular photoinduced electron transfer process. J Photochem Photobiol A Chem 260:39. doi:10.1016/j.jphotochem.2013.03.013
12. Huang D, Chen Y, Zhao J (2012) Access to a large stokes shift in functionalized fused coumarin derivatives by increasing the geometry relaxation upon photoexcitation: an experimental and theoretical study. Dyes Pigments 95:732. doi:10.1016/j.dyepig.2012.04.024
13. Schiedel M, Briehn C, Bäuerle P (2001) Single-compound libraries of organic materials: parallel synthesis and screening of fluorescent dyes. Angew Chem Int Ed 40:4677. doi:10.1002/1521-3773(20011217)40:24<4677
14. Xie L, Chen Y, Wu W, Guo H, Zhao J, Yu X (2012) Fluorescent coumarin derivatives with large stokes shift, dual emission and solid state luminescent properties: an experimental and theoretical study. Dyes Pigments 92:1361. doi:10.1016/j.dyepig.2011.09.023
15. Das S, Sarkar M (2011) Solvation and rotational relaxation of coumarin 153 and 4-aminophthalimide in a new hydrophobic ionic liquid: role of N–H…F interaction on solvation dynamics. Chem Phys Lett 515:23. doi:10.1016/j.cplett.2011.08.089
16. Mannekutla J, Mulimani B, Inamdar S (2008) Solvent effect on absorption and fluorescence spectra of coumarin laser dyes: evaluation of ground and excited state dipole moments. Spectrochim Acta A Mol Biomol Spectrosc 69:419. doi:10.1016/j.saa.2007.04.016
17. Kaholek M, Hrdlovic P (1997) Spectral properties of coumarin derivatives substituted at position 3. Effect of polymer matrix. J Photochem Photobiol A Chem 2–3:283. doi:10.1016/S1010-6030(97)00081-6
18. Toshiyuki I, Atsuya M, Yoshihiro S, Tomoo S, Yoshinobu N, Tatsuo A (2010) Excited-state intramolecular proton transfer of naphthalene-fused 2-(2′-Hydroxyaryl) benzazole family. J Phys Chem A 114:1603. doi:10.1021/jp904370t
19. Zhou S, Jia J, Gao J, Han L, Li Y, Sheng W (2010) The one-pot synthesis and fluorimetric study of 3-(2-benzothiazolyl)coumarins. Dyes Pigments 86:123. doi:10.1016/j.dyepig.2009.12.005
20. Lakowicz J (1999) Principles of fluorescence spectroscopy, 2nd edn. Kluwer Academic/Plenum Publishers, New York, p 75
21. Cossi M, Barone V, Cammi R, Tomasi J (1996) Ab initio study of solvated molecules: a new implementation of the polarizable continuum model. Chem Phys Lett 255:327–335. doi:10.1016/0009-2614(96)00349-1
22. Tomasi J, Mennucci B, Cammi R (2005) Quantum mechanical continuum solvation models. Chem Rev 105:2999–3093. doi:10.1021/cr9904009
23. Copeland R (1943) The preparation and reactions of 2-benzimidazolecarboxylic acid and 2-benzimidazoleacetic acid. J Am Chem Soc 65:1072. doi:10.1021/ja01246a019
24. Frisch MJ, Trucks GW, Schlegel HB, et al. (2009) Gaussian 09 C.01

25. Treutler O, Ahlrichs R (1995) Efficient molecular numerical integration schemes. J Chem Phys 102:346. doi:10.1063/1.469408
26. Becke AD (1993) A new mixing of hartree–fock and local density-functional theories. J Chem Phys 98:1372. doi:10.1063/1.464304
27. Lee C, Yang W, Parr RG (1988) Development of the colle-salvetti correlation-energy formula into a functional of the electron density. Phys Rev B 37:785–789. doi:10.1103/PhysRevB.37.785
28. Hehre WJ (1976) Ab initio molecular orbital theory. Acc Chem Res 9:399–406. doi:10.1021/ar50107a003
29. Bauernschmitt R, Ahlrichs R (1996) Treatment of electronic excitations within the adiabatic approximation of time dependent density functional theory. Chem Phys Lett 256:454–464. doi:10.1016/0009-2614(96)00440-X
30. Furche F, Rappoport D (2005) Computational photochemistry (Google eBook). 368
31. Gabe Y, Ueno T, Urano Y et al (2006) Tunable design strategy for fluorescence probes based on 4-substituted BODIPY chromophore: improvement of highly sensitive fluorescence probe for nitric oxide. Anal Bioanal Chem 386:621–626. doi:10.1007/s00216-006-0587-y
32. Furche F, Ahlrichs R (2002) Adiabatic time-dependent density functional methods for excited state properties. J Chem Phys 117:7433. doi:10.1063/1.1508368
33. Leszczynski J, Shukla M (2009) Practical aspects of computational chemistry: methods, concepts and applications (Google eBook). 484
34. Scalmani G, Frisch MJ, Mennucci B et al (2006) Geometries and properties of excited states in the gas phase and in solution: theory and application of a time-dependent density functional theory polarizable continuum model. J Chem Phys 124:94107. doi:10.1063/1.2173258
35. Valeur B, Berberan-Santos MN (2013) Molecular fluorescence: principles and applications (Google eBook), 2 nd. 500.